Tracing *CP* violation in the production of top quark pairs by multiple TeV proton-proton collisions

Werner Bernreuther

Institut für Theoretische Physik, Physikzentrum,
Rheinisch-Westfälische Technische Hochschule Aachen, 52056 Aachen, Germany

Arnd Brandenburg

Stanford Linear Accelerator Center, P.O. Box 4349, Stanford, California 94309

We investigate the possibilities of searching for nonstandard *CP* violation in $pp \rightarrow t\bar{t}X$ at multiple TeV collision energies. A general kinematic analysis of the underlying partonic production processes $gg \rightarrow t\bar{t}$ and $q\bar{q} \rightarrow t\bar{t}$ in terms of their density matrices is given. We evaluate the *CP*-violating parts of these matrices in two-Higgs-doublet extensions of the standard model (SM) and give results for *CP* asymmetries at the parton level. We show that these asymmetries can be traced by measuring suitable observables constructed from energies and momenta of the decay products of t and $\bar{t}$. We find *CP*-violating effects to be of the order of 10^{-3} and show that possible contaminations induced by SM interactions are safely below the expected signals.

I. INTRODUCTION

A high energy and high luminosity proton-proton collider, such as the planned Large Hadron Collider (LHC) at CERN, would be capable of producing millions of top quarks and top antiquarks. This would offer the unique possibility to explore in detail the physics of these quarks, which have not been discovered yet, but for whose existence there is indirect evidence [1]. Specifically, since the top quark is known to be heavy, $m_t > 113$ GeV [2], precision studies based on large samples of $t\bar{t}$ events may serve as a probe, through sizable top-Yukawa couplings, to the electroweak symmetry-breaking sector (Higgs sector for short). This sector may have a richer structure than the one conceived in the standard model (SM), as is the case in many of its extensions. As a consequence a number of new phenomena may exist. A particularly intriguing one is a new "source" of *CP* violation provided by the Higgs sector[1] which is unrelated to the Kobayashi-Maskawa phase [3]. This is possible already in the two-Higgs-doublet extensions of the SM [5–7]: here neutral Higgs boson exchange leads to *CP*-violating effects in fermionic amplitudes, and these effects would show up most pronouncedly in reactions involving top quarks [8–11]. The subject of this paper is to investigate in detail[2] the manifestation and the magnitude of neutral Higgs particle *CP* violation in $pp \rightarrow t\bar{t}X$. (For other studies on *CP* violation in top quark production and decay see [12–25].)

The outline of our paper is as follows. In Sec. II we give a general kinematic analysis of the reactions $gg \rightarrow t\bar{t}$

and $q\bar{q} \rightarrow t\bar{t}$ which are the leading partonic processes in $pp \rightarrow t\bar{t}X$. We study these reactions in terms of their production density matrices and describe the properties of these matrices under various symmetry transformations including *CP* transformations. In Sec. III we evaluate the *CP*-violating parts of the density matrices in a specific model, namely, the two-Higgs doublet extensions of the SM with *CP*-nonconserving neutral Higgs boson exchange. Correlations which are sensitive to *CP* violation at the parton level are identified and results for their expectation values are presented. In Sec. IV we show that these *CP* asymmetries can be traced in $pp \rightarrow t\bar{t}X$ by looking at simple observables which involve energies and/or momenta of the decay products of t and $\bar{t}$. Moreover, possible contaminations by *CP*-conserving interactions are discussed and shown to be much smaller than the expected signals. In an appendix we list the analytic results of our calculations.

II. PRODUCTION DENSITY MATRICES FOR $gg \rightarrow t\bar{t}$ AND $q\bar{q} \rightarrow t\bar{t}$

Because a heavy top quark has an extremely short lifetime ($\tau_t < 10^{-23}$ s if $m_t > 100$ GeV), the polarization of and spin-spin correlations between t and $\bar{t}$ are not severely diluted by hadronization [34]. These are "good" observables in the sense that effects involving the spins of t and $\bar{t}$ can be treated perturbatively. Therefore we will discuss the reaction $pp \rightarrow t\bar{t}X$ in terms of production density matrices for the underlying partonic processes. We will consider only unpolarized pp collisions. At LHC energies $t\bar{t}$ pairs are produced mainly by gluon-gluon fusion. This reaction dominates over quark-antiquark annihilation into $t\bar{t}$. We will first discuss the (unnormalized) production density matrix for the reaction $g(p_1) + g(p_2) \rightarrow t(k_1) + \bar{t}(k_2)$ in the gluon-gluon center of mass system. It is defined by

---

[1]This source was shown to be of interest in attempts to explain the cosmological baryon asymmetry [4].

[2]A short account of our work was given in [11].

$$R^g_{\alpha_1\alpha_2,\beta_1\beta_2}(\mathbf{p},\mathbf{k}) = N_g^{-1} \sum_{\text{colors,gluon spin}} \langle t(k_1,\alpha_1),\bar{t}(k_2,\beta_1)|T|g(p_1),g(p_2)\rangle^* \langle t(k_1,\alpha_2),\bar{t}(k_2,\beta_2)|T|g(p_1),g(p_2)\rangle \, , \qquad (2.1)$$

where α,β are spin indices, $\mathbf{p}=\mathbf{p}_1$, $\mathbf{k}=\mathbf{k}_1$, and $N_g=256$. We sum here over the gluon spins and colors since we are only interested in analyzing the polarizations of the t and $\bar{t}$ and their spin-spin correlations. The matrix R^g can be decomposed in the spin spaces of t and $\bar{t}$ as

$$R^g = A^g \mathbf{1}\otimes\mathbf{1} + B_i^{g+}\sigma^i\otimes\mathbf{1} + B_i^{g-}\mathbf{1}\otimes\sigma^i + C_{ij}^g\sigma^i\otimes\sigma^j \, . \qquad (2.2)$$

The first (second) factor in the tensor products of the 2×2 unit matrix $\mathbf{1}$ and of the Pauli matrices σ^i refers to the t ($\bar{t}$) spin space.

Because of rotational invariance, the functions $B_i^{g\pm}$ and C_{ij} can be further decomposed:

$$B_i^{g\pm} = b_{g1}^{\pm}\hat{p}_i + b_{g2}^{\pm}\hat{k}_i + b_{g3}^{\pm}\hat{n}_i \, ,$$

$$C_{ij} = c_{g0}\delta_{ij} + \epsilon_{ijl}(c_{g1}\hat{p}_l + c_{g2}\hat{k}_l + c_{g3}\hat{n}_l) + c_{g4}\hat{p}_i\hat{p}_j + c_{g5}\hat{k}_i\hat{k}_j + c_{g6}(\hat{p}_i\hat{k}_j + c_{g6}(\hat{p}_i\hat{k}_j + \hat{p}_j\hat{k}_i)$$

$$\qquad\qquad + c_{g7}(\hat{p}_i\hat{n}_j + \hat{p}_j\hat{n}_i) + c_{g8}(\hat{k}_i\hat{n}_j + \hat{k}_j\hat{n}_i) \, . \qquad (2.3)$$

Here the caret denotes a unit vector and $\mathbf{n}=\mathbf{p}\times\mathbf{k}$. The structure functions A^g, $b_{gi}^{\pm}$, and c_{gi} depend only on $\hat{s}=(p_1+p_2)^2$ and on the cosine of the scattering angle $z=\hat{\mathbf{p}}\cdot\hat{\mathbf{k}}$.

Next we discuss the properties of R^g under various symmetry transformations. Since the initial gg state is Bose symmetric, R^g must satisfy

$$R^g(-\mathbf{p},\mathbf{k}) = R^g(\mathbf{p},\mathbf{k}) \, . \qquad (2.4)$$

The initial gg state, when averaged over colors and spins, is a CP eigenstate in its center-of-mass system. It is therefore possible to classify the individual terms in R^g according to their CP transformation properties. If the interactions were CP invariant, the matrix R^g would have to satisfy

$$R^g_{\beta_1\beta_2,\alpha_1\alpha_2}(\mathbf{p},\mathbf{k}) = R^g_{\alpha_1\alpha_2,\beta_1\beta_2}(\mathbf{p},\mathbf{k}) \, . \qquad (2.5)$$

In Table I we give a complete list of the transformation

properties of the structure functions under P, CP, and exchange of the initial gluons ("Bose"). It is also instructive to collect the properties of these functions under time reversal (T) and CPT transformations neglecting, just for this purpose, non-Hermitian parts of the scattering matrix. To give an example, Table I is then to be read as follows: for a T-invariant interaction one has $b_{g3}^{\pm}(z) = -b_{g3}^{\pm}(z)$, i.e., $b_{g3}^{\pm}=0$ only at the Born level, whereas at higher orders absorptive parts render this function nonzero.

Because of Bose symmetry, the structure functions A^g, $b_{g2}^{\pm}$, c_{g0}, c_{g2}, c_{g4}, c_{g5}, and c_{g7} are even functions of z, the other functions are odd in z.

The contributions to R^g can be decomposed into a CP-even and a CP-odd part:

$$R^g = R^g_{\text{even}} + R^g_{CP} \, . \qquad (2.6)$$

As can be read off from Table I, the CP-even term R^g_{even} in general has the structure

$$R^g_{\text{even}} = A^g\mathbf{1}\otimes\mathbf{1} + (b_{g1}^{\text{even}}\hat{p}_i + b_{g2}^{\text{even}}\hat{k}_i + b_{g3}^{\text{even}}\hat{n}_i)(\sigma^i\otimes\mathbf{1} + \mathbf{1}\otimes\sigma^i)$$

$$\qquad + [c_{g0}\delta_{ij} + c_{g4}\hat{p}_i\hat{p}_j + c_{g5}\hat{k}_i\hat{k}_j + c_{g6}(\hat{p}_i\hat{k}_j + \hat{p}_j\hat{k}_i) + c_{g7}(\hat{p}_i\hat{n}_j + \hat{p}_j\hat{n}_i) + c_{g8}(\hat{k}_i\hat{n}_j + \hat{k}_j\hat{n}_i)]\sigma^i\otimes\sigma^j \, . \qquad (2.7)$$

Nonzero b_{g1}^{even}, b_{g2}^{even}, c_{g7}, c_{g8} can be induced only by parity-violating interactions, c_{g7}, c_{g8} need in addition absorptive parts in the scattering amplitude when the interactions are CPT invariant. The structure function b_{g3}^{even} can only get contributions from absorptive parts induced by parity-invariant interactions. The CP-odd term R^g_{CP} reads

$$R^g_{CP} = (b_{g1}^{CP}\hat{p}_i + b_{g2}^{CP}\hat{k}_i + b_{g3}^{CP}\hat{n}_i)(\sigma^i\otimes\mathbf{1} - \mathbf{1}\otimes\sigma^i) + \epsilon_{ijk}(c_{g1}\hat{p}_i + c_{g2}\hat{k}_i + c_{g3}\hat{n}_i)\sigma^j\otimes\sigma^k \, . \qquad (2.8)$$

CP-violating interactions which are also parity violating can give contributions to b_{g1}^{CP}, b_{g2}^{CP}, c_{g1}, c_{g2}. Nonzero b_{g1}^{CP}, b_{g2}^{CP} require in addition absorptive parts. C- and CP-violating interactions can induce nonvanishing structure functions b_{g3}^{CP}, c_{g3}, where $c_{g3}\neq0$ requires in addition absorptive parts.

The above discussion of the transformation properties of the structure functions holds to all orders of perturbation theory.

The production density matrix R^q for $q\bar{q}\to t\bar{t}$ is defined in complete analogy to (2.1) as

$$R^q_{\alpha_1\alpha_2,\beta_1\beta_2}(\mathbf{p},\mathbf{k}) = N_q^{-1} \sum_{\text{colors},q\bar{q}\text{ spins}} \langle t(k_1,\alpha_1),\bar{t}(k_2,\beta_1)|T|q(p_1),\bar{q}(p_2)\rangle^* \langle t(k_1,\alpha_2),\bar{t}(k_2,\beta_2)|T|q(p_1),\bar{q}(p_2)\rangle \, , \qquad (2.9)$$

TABLE I. Transformation properties of the structure functions defined in (2.2) and (2.3).

	CP	P	T (Im T =0)	CPT (Im T =0)	"Bose"
$A^g(z)$	$A^g(z)$	$A^g(z)$	$A^g(z)$	$A^g(z)$	$A^g(-z)$
$b_{g1}^\pm(z)$	$b_{g1}^\mp(z)$	$-b_{g1}^\pm(z)$	$b_{g1}^\pm(z)$	$b_{g1}^\mp(z)$	$-b_{g1}^\pm(-z)$
$b_{g2}^\pm(z)$	$b_{g2}^\mp(z)$	$-b_{g2}^\pm(z)$	$b_{g2}^\pm(z)$	$b_{g2}^\mp(z)$	$b_{g2}^\pm(-z)$
$b_{g3}^\pm(z)$	$b_{g3}^\mp(z)$	$b_{g3}^\pm(z)$	$-b_{g3}^\pm(z)$	$-b_{g3}^\mp(z)$	$-b_{g3}^\pm(-z)$
$c_{g0}(z)$	$c_{g0}(z)$	$c_{g0}(z)$	$c_{g0}(z)$	$c_{g0}(z)$	$c_{g0}(-z)$
$c_{g1}(z)$	$-c_{g1}(z)$	$-c_{g1}(z)$	$-c_{g1}(z)$	$c_{g1}(z)$	$-c_{g1}(-z)$
$c_{g2}(z)$	$-c_{g2}(z)$	$-c_{g2}(z)$	$-c_{g2}(z)$	$c_{g2}(z)$	$c_{g2}(-z)$
$c_{g3}(z)$	$-c_{g3}(z)$	$c_{g3}(z)$	$c_{g3}(z)$	$-c_{g3}(z)$	$-c_{g3}(-z)$
$c_{g4}(z)$	$c_{g4}(z)$	$c_{g4}(z)$	$c_{g4}(z)$	$c_{g4}(z)$	$c_{g4}(-z)$
$c_{g5}(z)$	$c_{g5}(z)$	$c_{g5}(z)$	$c_{g5}(z)$	$c_{g5}(z)$	$c_{g5}(-z)$
$c_{g6}(z)$	$c_{g6}(z)$	$c_{g6}(z)$	$c_{g6}(z)$	$c_{g6}(z)$	$-c_{g6}(-z)$
$c_{g7}(z)$	$c_{g7}(z)$	$-c_{g7}(z)$	$-c_{g7}(z)$	$-c_{g7}(z)$	$c_{g7}(-z)$
$c_{g8}(z)$	$c_{g8}(z)$	$-c_{g8}(z)$	$-c_{g8}(z)$	$-c_{g8}(z)$	$-c_{g8}(-z)$

where $N_q = 36$. The decomposition of R^q in the spin spaces of t and $\bar{t}$ is exactly the same as for R^g [Eq. (2.2), (2.3)] as is the splitting into CP-even and odd terms [Eqs. (2.6)–(2.8)]. The transformation properties of the structure functions $A^q, \ldots, c_{q8}$ of R^q are the same as the respective ones for $A^g, \ldots, c_{g8}$ of R^g given in Table I. Thus all conclusions derived from these transformation properties, except those from Bose symmetry, of course, are also valid for the structure functions of R^q.

III. *CP* VIOLATION AND DENSITY MATRICES IN TWO-HIGGS-DOUBLET MODELS

Up to now our discussion has been independent of any specific model. Suffice it to say that the Kobayashi-Maskawa mechanism of *CP* violation [3] induces only tiny effects in the flavor-diagonal reactions of Sec. II. In the following we will concentrate on *CP*-violating effects generated by two-Higgs-doublet extensions of the SM with *CP* violation in the scalar potential [6]. We briefly recall the features of these models relevant for us. *CP* violation in the scalar potential induces mixing of *CP*-even and -odd scalars, thus leading to three physical mass eigenstates $|\varphi_j\rangle$ ($j = 1,2,3$) with no definite *CP* parity. That means, these bosons couple both to scalar and pseudoscalar fermionic currents. For the top quark these couplings are (in the notation of [8])

$$\mathcal{L}_Y = -(\sqrt{2}\, G_F)^{1/2} \sum_{j=1}^{3} (a_{jt}\, m_t \bar{t}t + \tilde{a}_{jt}\, m_t \bar{t}i\gamma_5 t)\varphi_j \ ,$$

(3.1)

where G_F is Fermi's constant, m_t is the top mass,

$$a_{jt} = d_{2j}/\sin\beta, \quad \tilde{a}_{jt} = -d_{3j}\cot\beta \ ,$$

(3.2)

$\tan\beta = v_2/v_1$ is the ratio of vacuum expectation values of the two doublets, and d_{2j}, d_{3j} are the matrix elements of a 3×3 orthogonal matrix which describes the mixing of the neutral states [8]. In the following we assume that the couplings and masses of $\varphi_{2,3}$ are such that their effect on all quantities discussed below is negligible. Then the

measure of *CP* violation generated by $\varphi \equiv \varphi_1$ exchange in flavor-diagonal reactions such as $gg \to t\bar{t}, q\bar{q} \to t\bar{t}$ is

$$\gamma_{CP} \equiv -a\tilde{a} = d_{21}d_{31}\cot\beta/\sin\beta \ ,$$

(3.3)

where we have put $a = a_{1t}$, $\tilde{a} = \tilde{a}_{1t}$. So far, data from low energy phenomenology, in particular the experimental upper bounds on the electric dipole moments of the neutron [26] and of the electron [27] do not severely constrain this parameter: γ_{CP} may be of order one. We note here that the couplings of the φ_j to quarks and leptons induce *CP* violation already at the Born level. The especially interesting case of a Higgs boson φ decaying into $t\bar{t}$ was shown in [11] to lead to *CP*-violating spin-spin correlations which may be as large as 0.5. (For other discussions of the *CP* properties of neutral Higgs bosons see [28–33].)

We will now discuss the structure of the matrices R_{CP}^g and R_{CP}^q in these models. The Higgs boson contributions to the processes $gg \to t\bar{t}$ and $q\bar{q} \to t\bar{t}$ discussed in Sec. II are shown, together with the leading SM diagrams, in Figs. 1 and 2. Since the *CP*-nonconserving neutral Higgs exchange is, in particular, parity violating, the relations

$$R_{CP}^{g(q)}(-\mathbf{p}, -\mathbf{k}) = -R_{CP}^{g(q)}(\mathbf{p}, \mathbf{k})$$

(3.4)

hold as long as R_{CP} results from interference of these Higgs exchange amplitudes with amplitudes from parity-invariant interactions. This forces b_{g3}^{CP}, c_{g3} and b_{q3}^{CP}, c_{q3} to be zero in these models. Furthermore, the virtual intermediate gluon produced by annihilation of unpolarized q and $\bar{q}$ cannot have a vector polarization. Thus the contributions of Fig. 2 to R^q are invariant with respect to the substitution $\mathbf{p} = \mathbf{p}_1 \to -\mathbf{p}$. Hence the structures of R_{CP}^g and R_{CP}^q are the same; the functions b_{g1}^{CP}, c_{g1}, b_{q1}^{CP}, c_{q1} of Eq. (2.8) are odd under $z \to -z$, whereas $b_{g2}^{CP}, c_{g2}, b_{q2}^{CP}, c_{q2}$
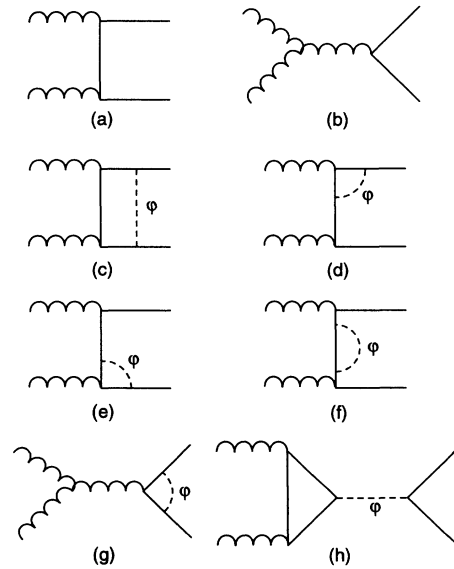

FIG. 1. Born level QCD and φ exchange Feynman diagrams which contribute to the production density matrix for $gg \to t\bar{t}$. Diagrams with crossed gluons are not shown.
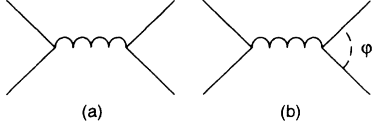
FIG. 2. Born level QCD and relevant φ exchange Feynman diagrams for $q\bar{q} \rightarrow t\bar{t}$.

are even functions of z.

The explicit results for the matrices R^g and R^q evaluated from the diagrams of Figs. 1 and 2, respectively, are given in the Appendix. The width of φ must be taken into account in the calculation of R^g if $\varphi > 2m_t$, since in that case the contribution from Fig. 1(h) can become resonant. Because for $\varphi > 2m_t$ the width of φ is not very small as compared to its mass it is important to note that the narrow width approximation cannot be applied in this case.

In view of the above discussion it is now very easy to identify the correlations at the parton level which trace the various CP-odd parts of the production density matrices. The expectation value of an observable $\mathcal{O}$ for the respective parton reactions is defined as

$$\langle \mathcal{O} \rangle_i = \frac{\int_{-1}^{1} dz\, \mathrm{tr}(R^i \mathcal{O})}{4 \int_{-1}^{1} dz\, A^i} \quad (i = g, q) . \tag{3.5}$$

The contributions of the functions $b_{g1,g2}^{CP}, b_{q1,q2}^{CP}$ are picked up by taking expectation values of

$$\hat{\mathbf{k}} \cdot (\mathbf{s}_+ - \mathbf{s}_-) f_e(z) \tag{3.6}$$

or

$$\hat{\mathbf{p}} \cdot (\mathbf{s}_+ - \mathbf{s}_-) f_o(z) , \tag{3.7}$$

or linear combinations thereof, where $\mathbf{s}_+, \mathbf{s}_-$ are the spin operators of t and $\bar{t}$, respectively, $f_e(z)$ is an even function of z and $f_o(z)$ is odd in z. One has, for example,

$$\langle \hat{\mathbf{k}} \cdot (\mathbf{s}_+ - \mathbf{s}_-) \rangle_g = \frac{4 \int_{-1}^{1} dz (z b_{g1}^{CP} + b_{g2}^{CP})}{4 \int_{-1}^{1} dz\, A^g} , \tag{3.8}$$
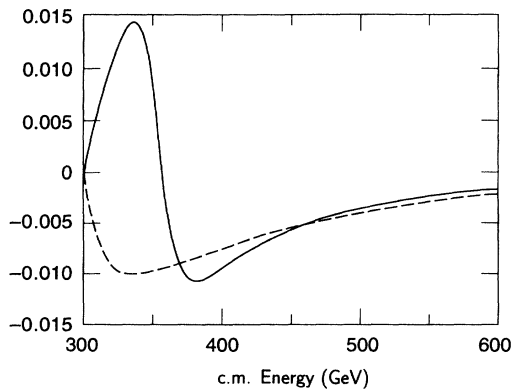

FIG. 3. Expectation value $\langle \hat{\mathbf{k}} \cdot (\mathbf{s}_+ - \mathbf{s}_-) \rangle_g$ as a function of the parton c.m. energy for $m_\varphi = 100$ GeV (dashed curve) and $m_\varphi = 350$ GeV (solid curve).
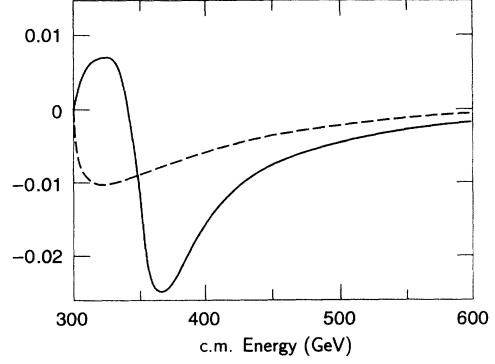

FIG. 4. Expectation value $\langle \hat{\mathbf{k}} \cdot (\mathbf{s}_+ \times \mathbf{s}_-) \rangle_g$ for the same choice of Higgs boson masses as in Fig. 3.

and likewise for $\langle \hat{\mathbf{k}} \cdot (\mathbf{s}_+ - \mathbf{s}_-) \rangle_q$.

The result of the basic longitudinal polarization asymmetry $\langle \hat{\mathbf{k}} \cdot (\mathbf{s}_+ - \mathbf{s}_-) \rangle_g$ is plotted in Fig. 3 as a function of the parton c.m. energy for $m_t = 150$ GeV and two values of the Higgs boson mass: The dashed curve corresponds to $m_\varphi = 100$ GeV and $\gamma_{CP} = 1$. For m_φ of the order of $2m_t$ or larger, the shape of the resulting graph depends, for fixed m_φ, on the strength of the Higgs couplings $a, \tilde{a}$ and on the couplings to $W^+ W^-$, ZZ determining the width of the φ. [See Eq. (A10) for details.] For the solid line we have chosen $m_\varphi = 350$ GeV, $|a| = |\tilde{a}| = \gamma_{CP} = 1$, and $\Gamma_\varphi = 47$ GeV. The asymmetry $\langle \hat{\mathbf{k}} \cdot (\mathbf{s}_- - \mathbf{s}_+) \rangle$ corresponds to the asymmetry $\Delta N_{LR} = [N(t_L \bar{t}_L) - N(t_R \bar{t}_R)]/(\text{all } t\bar{t})$ studied in [10]. We reproduce the numerical results of [10] for ΔN_{LR} if we neglect Γ_φ and use $\gamma_{CP} = 1/\sqrt{2}$ which corresponds to the parameter $\mathrm{Im}(A^2) = \sqrt{2}$ used in [10].

The functions $c_{g1,g2}$, $c_{q1,q2}$ generate nonzero expectation values of the triple product correlations

$$\hat{\mathbf{k}} \cdot (\mathbf{s}_+ \times \mathbf{s}_-) h_e(z) , \tag{3.9}$$

$$\hat{\mathbf{p}} \cdot (\mathbf{s}_+ \times \mathbf{s}_-) h_o(z) , \tag{3.10}$$

and of their linear combinations, where h_e and h_o are even and odd functions of z, respectively. For example,
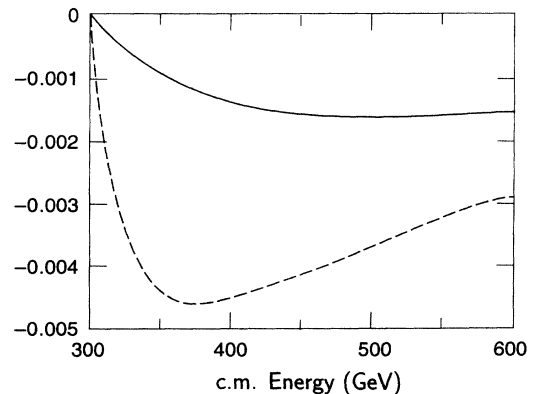

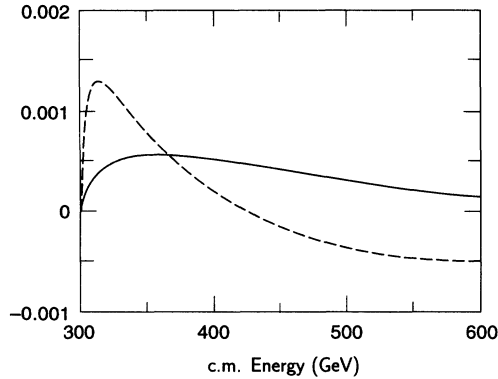FIG. 5. Same as Fig. 3, but for $\langle \hat{\mathbf{k}} \cdot (\mathbf{s}_+ - \mathbf{s}_-) \rangle_q$.

FIG. 6. Same as Fig. 4, but for $\langle \hat{\mathbf{k}} \cdot (\mathbf{s}_+ \times \mathbf{s}_-) \rangle_q$.

$$\langle \hat{\mathbf{k}} \cdot (\mathbf{s}_+ \times \mathbf{s}_-) \rangle_g = \frac{2\int_{-1}^{1} dz(zc_{g1} + c_{g2})}{4\int_{-1}^{1} dz \, A^g} . \quad (3.11)$$

In Fig. 4 we plot this basic *CP*-odd and *T*-odd spin-spin correlations with the same choice of parameters as in Fig. 3. It reaches values of up to about 2%.

For completeness we show in Figs. 5 and 6 the expectation values $\langle \hat{\mathbf{k}} \cdot (\mathbf{s}_+ - \mathbf{s}_-) \rangle_q$ and $\langle \hat{\mathbf{k}} \cdot (\mathbf{s}_+ \times \mathbf{s}_-) \rangle_q$, respectively, again for the same choice of parameters as in Fig. 3. Here the *CP* asymmetries get smaller with growing Higgs boson masses.

IV. *CP* OBSERVABLES FOR $pp \rightarrow t\bar{t}X$

The *CP*-violating spin-momentum correlations for t and $\bar{t}$ of the previous section must be traced in the final states into which t and $\bar{t}$ decay. In this section we discuss a few observables which allow us to do this. The charged lepton from $t \rightarrow Wb \rightarrow l^+ v_l b$ is an efficient analyzer of the top spin [35]. We will therefore consider only decay chains where at least one of the top quarks decays semileptonically. We shall use the SM decay density matrices as given in [16,18].

Observables in $pp \rightarrow t\bar{t}X$ cannot be classified as being even or odd with respect to *CP*, because the initial state is not a *CP* eigenstate. However, they can be classified as being T even or T odd (i.e., even or odd under reflection of momenta and spins). Their expectation values will in general be contaminated by contributions from *CP*-conserving interactions.

The asymmetries in the t and $\bar{t}$ polarizations in the production plane, as given in Eqs. (3.6) and (3.7), translate into T-even observables formed by energies and/or momenta of the final states. As an example we have investigated the expectation values of the two observables (another one was given in [10])

$$A_1 = E_+ - E_- , \quad (4.1)$$

$$A_2 = \mathbf{k}_{\bar{t}} \cdot l^+ - \mathbf{k}_t \cdot l^- . \quad (4.2)$$

Here $E_{\pm}, l^{\pm}$ are the energies and momenta of the leptons in $t \rightarrow l^+ v_l b$ and $\bar{t} \rightarrow l^- \bar{v}_l \bar{b}$ in the laboratory frame and $\mathbf{k}_{t(\bar{t})}$ is the top (antitop) momentum in this system.

To measure A_2, one has to select events where the t decays leptonically and the $\bar{t}$ hadronically, which in principle allow to reconstruct the $\bar{t}$ momentum [36], and vice versa. We will give explicit expressions for the expectation values of A_1 and A_2 below when we discuss contaminations by *CP*-conserving interactions. In calculating these expectation values we have used the narrow width approximation for the top: because the top width is much smaller than its mass (in view of the experimental upper bound on m_t which is of the order of 200 GeV), the approximation of the on-shell production of t and $\bar{t}$ followed by their weak decays yields a good description of the reactions considered here. We also neglected *CP* violation in the decays of t and $\bar{t}$ (for comments on this, see [11]). For the parton distributions entering the calculation of expectation values in pp collisions we have used the parametrization of [37]. In order to assess the statistical sensitivity of the observables A_1 and A_2, we have computed the signal-to-noise ratios $\langle A_i \rangle / \Delta A_i (i = 1,2)$ for Higgs boson masses 100 GeV $\leq m_{\varphi} \leq 450$ GeV both for $\sqrt{s} = 15$ TeV (LHC) and $\sqrt{s} = 40$ TeV. Here $\Delta A_i = \sqrt{\langle A_i^2 \rangle - \langle A_i \rangle^2}$ denotes the width of the distribution of A_i. We present our results in Figs. 7 and 8 for the same parameter set as used in calculating the partonic asymmetries, that is, $a = -\bar{a} = 1$, $\hat{g}_{VV} = 1$ [for the definition of $\hat{g}_{VV}$ see the Appendix, Eq. (A9)]. We integrate here over the whole phase space. Both observables have signal-to-noise ratios of order 10^{-3}. LHC offers larger effects due to the fact that $\Delta A_{1,2}$ is larger for $\sqrt{s} = 40$ TeV.

If both t and $\bar{t}$ decay leptonically one can look at the T-odd observable

$$T_2 = (\mathbf{b} - \bar{\mathbf{b}}) \cdot (l^+ \times l^-) \quad (4.3)$$

where $\mathbf{b}, \bar{\mathbf{b}}$ denote the momenta of the b and $\bar{b}$ jets in the laboratory frame. (This observable was also discussed in [11].) The expectation value of T_2 traces the spin-spin correlations of (3.9) and (3.10). In Fig. 9 we show the signal-to-noise ratio as a function of the Higgs boson mass for this observable, again with the same choice of parameters as for $A_{1,2}$. The effect is also of the order of 10^{-3}.
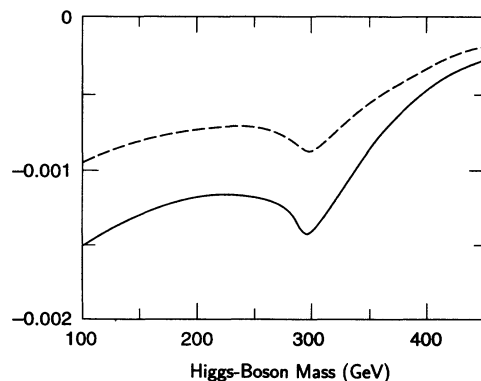

FIG. 7. Signal-to-noise ratio for the observable A_1 [defined in (4.1)] as a function of the Higgs boson mass m_{φ} for proton-proton c.m. energies $\sqrt{s} = 15$ TeV (solid curve) and $\sqrt{s} = 40$ TeV (dashed curve). Here $m_t = 150$ GeV, $a = -\bar{a} = 1$, $\hat{g}_{VV} = 1$.

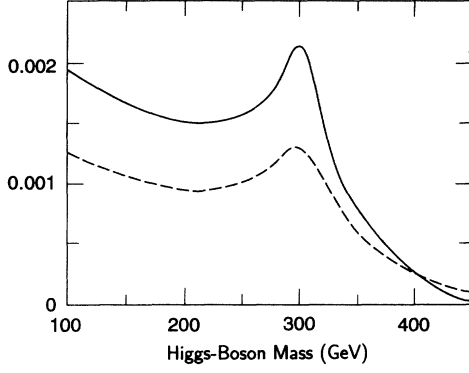FIG. 8. Same as Fig. 7, but for the observable A_2 [defined in (4.2)].

FIG. 9. Same as Fig. 7, but for the observable T_2 [defined in (4.3)].

We will now discuss in some detail possible contaminations of the observables $A_{1,2}$ and T_2 due to CP-conserving interactions. Such contaminations arise in particular because the pp initial state is not a CP eigenstate. One can give general arguments why these contaminations should be small. Most importantly, the dominant subprocess is gluon fusion which does not induce any CP-conserving contributions to our observables (cf. [11] and below). Furthermore, T-odd observables such as T_2 do not receive contributions from CP-invariant interactions at the Born level but only from absorptive parts. The main background in this case comes from order α_s^3 and order $\alpha_s^2 \alpha_{weak}$ absorptive parts in $q\bar{q} \rightarrow t\bar{t}$ which generate nonzero functions b_3^{even} in R^q. However, numerical simulations show that these contributions are smaller than 10^{-6}, i.e., about 3 orders of magnitude
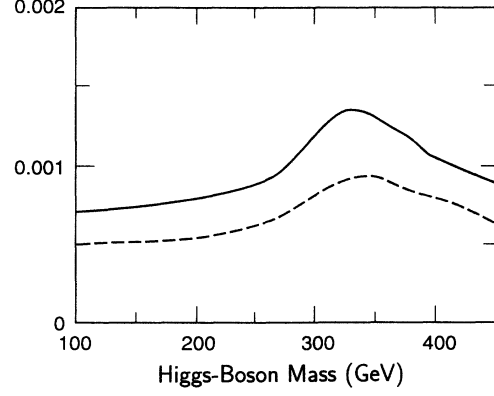
smaller than the signal shown in Fig. 9. Potentially more dangerous are CP-even contributions to A_1 and A_2, because, as will be shown below, they can already be generated by weak interactions at the Born level.

Integrating over the whole phase space we can actually give explicitly analytic formulas for the expectation values of A_1 and A_2 in terms of the structure functions. This is very illuminating for identifying possible contaminations. We have carried out our calculations within the naive parton model (which neglects intrinsic transverse momenta of the incoming partons) and restricted ourselves again to gg and $q\bar{q}$ initial states. Furthermore, we have used the narrow width approximation described above and have taken into account only the SM decays of t and $\bar{t}$. Then we find

$$\langle A_1 \rangle = \frac{1}{\sigma} \frac{1}{2s} \frac{g(m_W^2/m_t^2)}{4\pi}$$

$$\times \left[\int_0^1 dx_1 \frac{N_g^p(x_1)}{x_1} \int_0^1 dx_2 \frac{N_g^p(x_2)}{x_2} \int_{-1}^1 dz\, \beta \frac{x_1+x_2}{2\sqrt{x_1 x_2}} \frac{E_1}{3} (zb_{g1}^{CP} + b_{g2}^{CP}) \right.$$

$$+ 2 \int_0^1 dx_1 \frac{N_q^p(x_1)}{x_1} \int_0^1 dx_2 \frac{N_{\bar{q}}^p(x_2)}{x_2} \int_{-1}^1 dz\, \beta \left[\frac{x_1+x_2}{2\sqrt{x_1 x_2}} \frac{E_1}{3} (zb_{q1}^{CP} + b_{q2}^{CP}) \right.$$

$$\left. \left. + \frac{x_1-x_2}{2\sqrt{x_1 x_2}} (E_1 \beta z A^q + \tfrac{1}{3} \{ [(1-z^2)m_t + z^2 E_1] b_{q1}^{even} + E_1 z b_{q2}^{even} \}) \right] \right] , \tag{4.4}$$

$$\langle A_2 \rangle = \frac{1}{\sigma} \frac{1}{2s} \frac{g(m_W^2/m_t^2)}{4\pi}$$

$$\times \left[\int_0^1 dx_1 \frac{N_g^p(x_1)}{x_1} \int_0^1 dx_2 \frac{N_g^p(x_2)}{x_2} \int_{-1}^1 dz\, \beta \left[-\frac{E_1^2 \beta}{3} (zb_{g1}^{CP} + b_{g2}^{CP}) \right. \right.$$

$$\left. + \frac{(x_1-x_2)^2}{4x_1 x_2} \frac{E_1 \beta}{3} (1-z^2)[(E_1 - m_t) zb_{g1}^{CP} + E_1 b_{g2}^{CP}] \right]$$

$$+ 2 \int_0^1 dx_1 \frac{N_q^p(x_1)}{x_1} \int_0^1 dx_2 \frac{N_{\bar{q}}^p(x_2)}{x_2} \int_{-1}^1 dz\, \beta \left[-\frac{E_1^2 \beta}{3} (zb_{q1}^{CP} + b_{q2}^{CP}) \right.$$

$$+ \frac{(x_1-x_2)^2}{4x_1 x_2} \frac{E_1 \beta}{3} (1-z^2)[(E_1 - m_t) zb_{q1}^{CP} + E_1 b_{q2}^{CP}]$$

$$\left. \left. + \frac{x_1^2 - x_2^2}{4x_1 x_2} \frac{m_t}{3} \{ [(1-z^2)E_1 + z^2 m_t] b_{q1}^{even} + m_t z b_{q2}^{even} \} \right] \right] . \tag{4.5}$$

Here σ is the total cross section for $pp \rightarrow t\bar{t}X$, s is the pp collision energy squared, $g(y) = (1+2y+3y^2)/(2+4y)$, $N_g^p, N_{q(\bar{q})}^p$ denote the gluon and quark (antiquark) distribution functions of the proton, E_1 is the energy of the top quark in the partonic c.m., and $\beta = (1 - m_t^2/E_1^2)^{1/2}$.

Equations (4.4) and (4.5) exhibit several interesting features. One can see explicitly that gluon fusion generates no *CP*-even contributions to the observables. Quark-antiquark annihilation produces several contaminations: In $\langle A_1 \rangle$ a term $\sim z A^q(z)$ appears which, after integrating over z, is nonzero only if $A^q(z)$ has a part which is odd in z; that is, if $q\bar{q} \rightarrow t\bar{t}$ has a forward-backward asymmetry. Such an asymmetry is induced in order α_s^3. (In [10] this potential source of contaminations was discussed.) Possibly more important are the terms b_{q1}^{even} and b_{q2}^{even} which appear in both expectation values above because these terms can be generated at the Born level via $q\bar{q} \rightarrow Z \rightarrow t\bar{t}$. We calculated their contributions and found that for both observables they are suppressed by more than 2 orders of magnitude in comparison to the signals shown in Figs. 7 and 8.

A future multiple TeV and high luminosity collider such as the LHC has the potential of producing more than $10^7 t\bar{t}$ pairs. If it were for statistics alone detection of effects of a few permil which we found might be feasible. More detailed (Monte Carlo) studies including judicious choices of phase space cuts are required in order to explore the possibility of enhancing the signals by some factor. A crucial issue will eventually be whether detector effects can be kept at the level of 10^{-3}.

V. CONCLUSIONS

In this paper we have studied the possibility of detecting *CP* violation in top quark pair production at future hadron colliders. We have given a general kinematic analysis of the underlying dominant partonic subprocesses and identified the relevant *CP* asymmetries at the parton level. We have further computed these asymmetries in two-Higgs doublet extensions of the SM where *CP* violation is generated through neutral Higgs boson exchange. Whereas at the parton level these models can induce asymmetries of the order of a few percent, realistic observables built up from energies and/or momenta of the final states into which the top quarks decay give signal-to-noise ratios of up to a few $\times 10^{-3}$. Contaminations by *CP*-conserving interactions were shown to be much smaller than the signals. Since the issue of *CP* violation is of fundamental interest detailed investigations of the experimental feasibility of an observation of these effects would certainly be worthwhile.

ACKNOWLEDGMENTS

APPENDIX

In this appendix we list our analytic results for the structure functions of the $t\bar{t}$ spin density matrix R^g defined in Eqs. (2.1)–(2.3) and decomposed into *CP*-even and *CP*-odd parts in Eqs. (2.6)–(2.8) and also the corresponding functions in R^q defined in (2.9). All calculations are carried out in the two-Higgs-doublet extensions of the SM described in Sec. III. The relevant Feynman diagrams are shown in Figs. 1(a)–1(h) for the process $gg \rightarrow t\bar{t}$ and in Figs. 2(a) and 2(b) for $q\bar{q} \rightarrow t\bar{t}$.

R^q is obtained very easily: The *CP*-even part is determined to good approximation by the Born diagram Fig. 2(a), whereas R_{CP}^q results from the interference of Fig. 2(b) (with couplings $a\tilde{a} = -\gamma_{CP}$) with Fig. 2(a). The nonzero *CP*-even structure functions of R^q read

$$A^q = \frac{g_s^4 [\beta^2(z^2-1)+2]}{18} ,$$

$$c_{q0} = \frac{g_s^4 \beta^2 (z^2-1)}{18} ,$$

$$c_{q4} = \frac{g_s^4}{9} , \tag{A1}$$

$$c_{q5} = \frac{g_s^4 \beta^2}{9} \left[\frac{\beta^2 z^2 E_1^2}{(E_1 + m_t)^2} + 1 \right] ,$$

$$c_{q6} = \frac{-g_s^4 \beta^2 z E_1}{9(E_1 + m_t)} .$$

Here and in the following g_s denotes the strong coupling constant, E_1 is the energy of the top quark in the c.m. system of the incoming partons, and $\beta = \sqrt{1 - m_t^2/E_1^2}$. Recall that $z = \hat{\mathbf{p}} \cdot \hat{\mathbf{k}}$.

The *CP*-odd contributions are

$$b_{q1}^{CP} = \frac{-m_t^3 \sqrt{2} \, G_F \gamma_{CP}}{8\pi^2} \frac{4g_s^4 E_1 \beta z}{9} \text{Im} G(\hat{s}) , \tag{A2}$$

$$b_{q2}^{CP} = \frac{m_t^3 \sqrt{2} \, G_F \gamma_{CP}}{8\pi^2} \frac{4g_s^4 E_1 \beta}{9} \left[\frac{(z^2-1)\beta^2 E_1}{E_1 + m_t} \right.$$
$$\left. + 1 \right] \text{Im} G(\hat{s}) , \tag{A3}$$

$$c_{q1} = \frac{m_t^3 \sqrt{2} \, G_F \gamma_{CP}}{8\pi^2} \frac{4g_s^4 E_1 \beta z}{9} \text{Re} G(\hat{s}) , \tag{A4}$$

$$c_{q2} = \frac{-m_t^3 \sqrt{2} \, G_F \gamma_{CP}}{8\pi^2} \frac{4g_s^4 E_1 \beta}{9} \left[\frac{(z^2-1)\beta^2 E_1}{E_1 + m_t} \right.$$
$$\left. + 1 \right] \text{Re} G(\hat{s}) . \tag{A5}$$

Here G_F is Fermi's constant and

$$G(\hat{s}) = \frac{-[m_\varphi^2 C_0(\hat{s},m_\varphi^2,m_t^2,m_t^2) + B_0(\hat{s},m_t^2,m_t^2) - B_0(m_t^2,m_\varphi^2,m_t^2)]}{\hat{s}\beta^2} ,$$ (A6)

where

$$C_0(\hat{s},m_\varphi^2,m_t^2,m_t^2) = \int \frac{d^4l}{i\pi^2} \frac{1}{l^2-m_\varphi^2+i\epsilon} \frac{1}{(l+k_1)^2-m_t^2+i\epsilon} \frac{1}{(l+k_1-p_1-p_2)^2-m_t^2+i\epsilon}$$ (A7)

is a standard three-point scalar integral which can be reduced to dilogarithms [38]. We note here that for the models of Sec. III all structure functions are ultraviolet finite. In particular, the scalar two-point functions B_0 show up in all our results only as differences of the form

$$B_0(q_1^2,m_1^2,m_t^2) - B_0(q_2^2,m_2^2,m_t^2)$$

$$= -\int_0^1 dx \ln \left[\frac{x^2 q_1^2 + x(m_t^2-m_1^2-q_1^2) + m_1^2 - i\epsilon}{x^2 q_2^2 + x(m_t^2-m_2^2-q_2^2) + m_2^2 - i\epsilon} \right] .$$ (A8)

This completes our results for the matrix R^q.

The computation of R^g is more involved since the contribution of Fig. 1(h) becomes resonant if $m_\varphi > 2m_t$. [Figure 1(h) actually represents four amplitudes: two CP-conserving ones with couplings a^2 and $\bar{a}^2$, respectively, and two CP-violating ones with coupling $a\bar{a}$.] The width of φ must therefore be taken into account in the φ propagator. We compute Γ_φ by summing the partial widths for $\varphi \to W^+W^-, ZZ, t\bar{t}$ in the two-Higgs doublet model which contains (3.1). At the Born level only the $CP = +1$ component of φ couples to W^+W^- and ZZ. The couplings are given by the respective SM couplings times the factor

$$\hat{g}_{VV} = (d_{11}\cos\beta + d_{21}\sin\beta) .$$ (A9)

Explicitly,

$$\Gamma_\varphi = \Gamma_W + \Gamma_Z + \Gamma_t ,$$

$$\Gamma_W = \Theta(m_\varphi - 2m_W) \frac{\hat{g}_{VV}^2 m_\varphi^3 \sqrt{2} G_F \beta_W}{16\pi} \left[\beta_W^2 + 12\frac{m_W^4}{m_\varphi^4} \right] ,$$ (A10)

$$\Gamma_Z = \Theta(m_\varphi - 2m_Z) \frac{\hat{g}_{VV}^2 m_\varphi^3 \sqrt{2} G_F \beta_Z}{8\pi} \left[\beta_Z^2 + 12\frac{m_Z^4}{m_\varphi^4} \right] ,$$

$$\Gamma_t = \Theta(m_\varphi - 2m_t) \frac{3m_\varphi m_t^2 \sqrt{2} G_F \beta_t}{8\pi} (\beta_t^2 a^2 + \bar{a}^2) .$$

Here we have used the notation $\beta_{W,Z,t} = (1 - 4m_{W,Z,t}^2/m_\varphi^2)^{1/2}$. In order to incorporate the resonance region we have determined R_{even}^g from the squared Born amplitudes Figs. 1(a) and 1(b), the interference of Fig. 1(a) with the CP-even amplitudes of Fig. 1(h), and the squared amplitudes of Fig. 1(h). We denote the Born contributions by a lower index "Born" and the other two contributions by a lower index "resonance" in the following. The results for the nonzero structure functions of R_{even}^g are

$$A^g = A^g_{\text{Born}} + A^g_{\text{resonance}} ,$$

$$A^g_{\text{Born}} = \frac{g_s^4(7+9\beta^2 z^2)}{192E_1^4(-1+\beta^2 z^2)^2} (E_1^4 + 2E_1^2 m_t^2 - 2m_t^4 - 2\beta^2 E_1^2 m_t^2 z^2 - \beta^4 E_1^4 z^4) ,$$

$$A^g_{\text{resonance}} = \frac{g_s^4}{(\hat{s}-m_\varphi^2)^2 + \Gamma_\varphi^2 m_\varphi^2} \left[-\frac{1}{16} \frac{m_t^3 \sqrt{2} G_F}{8\pi^2} \frac{m_t}{-1+\beta^2 z^2} \right.$$

$$\times \{2\hat{s}(a^2\beta^4 + \bar{a}^2)[\text{Re}C_0(\hat{s},m_t^2,m_t^2,m_t^2)(\hat{s}-m_\varphi^2)$$

$$+ \text{Im}C_0(\hat{s},m_t^2,m_t^2,m_t^2)\Gamma_\varphi m_\varphi] - 4a^2\beta^2(\hat{s}-m_\varphi^2)\}$$

$$+ \frac{3}{32} \left[\frac{m_t^3 \sqrt{2} G_F}{8\pi^2} \right]^2 [\hat{s}^3(a^2\bar{a}^2\beta^2 + \bar{a}^4)|C_0(\hat{s},m_t^2,m_t^2,m_t^2)|^2$$

$$\left. + \hat{s}(a^4\beta^2 + a^2\bar{a}^2)|2 - \hat{s}\beta^2 C_0(\hat{s},m_t^2,m_t^2,m_t^2)|^2] \right] ,$$ (A11)

$$c_{g0} = c_{g0,\text{Born}} + c_{g0,\text{resonance}} ,$$

$$c_{g0,\text{Born}} = \frac{-g_s^4(7+9\beta^2 z^2)}{192E_1^4(-1+\beta^2 z^2)^2} (E_1^4 - 2E_1^2 m_t^2 + 2m_t^4 - 2\beta^2 E_1^4 z^2 + 2\beta^2 E_1^2 m_t^2 z^2 + \beta^4 E_1^4 z^4) ,$$

$$c_{g0,\text{resonance}} = \frac{g_s^4}{(\hat{s}-m_\varphi^2)^2+\Gamma_\varphi^2 m_\varphi^2} \left[-\frac{1}{16} \frac{m_t^3\sqrt{2}\,G_F}{8\pi^2} \frac{m_t}{-1+\beta^2 z^2} \right.$$

$$\times \{ 2\hat{s}(a^2\beta^4-\bar{a}^2)[\text{Re}C_0(\hat{s},m_t^2,m_t^2,m_t^2)(\hat{s}-m_\varphi^2) $$

$$+ \text{Im}C_0(\hat{s},m_t^2,m_t^2,m_t^2)\Gamma_\varphi m_\varphi]-4a^2\beta^2(\hat{s}-m_\varphi^2)\} $$

$$+ \frac{3}{32}\left[\frac{m_t^3\sqrt{2}\,G_F}{8\pi^2}\right]^2 [\hat{s}^3(a^2\bar{a}^2\beta^2-\bar{a}^4)|C_0(\hat{s},m_t^2,m_t^2,m_t^2)|^2 $$

$$\left. + \hat{s}(a^4\beta^2-a^2\bar{a}^2)|2-\hat{s}\beta^2 C_0(\hat{s},m_t^2,m_t^2,m_t^2)|^2] \right] , \tag{A12}$$

$$c_{g4} = \frac{g_s^4\beta^2(7+9\beta^2 z^2)(1-z^2)}{96(-1+\beta^2 z^2)^2} , \tag{A13}$$

$$c_{g5} = c_{g5,\text{Born}} + c_{g5,\text{resonance}} ,$$

$$c_{g5,\text{Born}} = \frac{g_s^4\beta^2(7+9\beta^2 z^2)}{96E_1^2(E_1+m_t)^2(-1+\beta^2 z^2)^2}(E_1^4+2E_1^3 m_t-E_1^2 m_t^2-4E_1 m_t^3-2m_t^4-2\beta^2 E_1^3 m_t z^2-2\beta^2 E_1^2 m_t^2 z^2-\beta^4 E_1^4 z^4) ,$$

$$c_{g5,\text{resonance}} = \frac{g_s^4}{(\hat{s}-m_\varphi^2)^2+\Gamma_\varphi^2 m_\varphi^2}\left[\frac{1}{16}\frac{m_t^3\sqrt{2}\,G_F}{8\pi^2}\frac{m_t}{-1+\beta^2 z^2}\right.$$

$$\times \{4\hat{s}a^2\beta^4[\text{Re}C_0(\hat{s},m_t^2,m_t^2,m_t^2)(\hat{s}-m_\varphi^2) $$

$$+ \text{Im}C_0(\hat{s},m_t^2,m_t^2,m_t^2)\Gamma_\varphi m_\varphi]-8a^2\beta^2(\hat{s}-m_\varphi^2)\} $$

$$- \frac{3}{32}\left[\frac{m_t^3\sqrt{2}\,G_F}{8\pi^2}\right]^2 [2\hat{s}^3 a^2\bar{a}^2\beta^2|C_0(\hat{s},m_t^2,m_t^2,m_t^2)|^2 $$

$$\left. + 2\hat{s}a^4\beta^2|2-\hat{s}\beta^2 C_0(\hat{s},m_t^2,m_t^2,m_t^2)|^2] \right] , \tag{A14}$$

$$c_{g6} = \frac{g_s^4\beta^4 z E_1(7+9\beta^2 z^2)(z^2-1)}{96(E_1+m_t)(-1+\beta^2 z^2)^2} . \tag{A15}$$

The scalar three point function C_0 appearing in Eqs. (A11), (A12), and (A14) is given by

$$C_0(\hat{s},m_t^2,m_t^2,m_t^2) = \int \frac{d^4 l}{i\pi^2} \frac{1}{l^2-m_t^2+i\epsilon} \frac{1}{(l-p_1)^2-m_t^2+i\epsilon} \frac{1}{(l-p_1-p_2)^2-m_t^2+i\epsilon} . \tag{A16}$$

Numerically, R_{even}^g is dominated by the Born contributions. This completes our discussion of R_{even}^g.

The *CP*-violating part R_{CP}^g results from the interference of the Born diagrams with the amplitudes of Figs. 1(c)–1(h) (with couplings $a\bar{a} = -\gamma_{CP}$) and the interference of the *CP*-even and -odd amplitudes of Fig. 1(h). We found that if m_φ is of the order of $2m_t$ or larger, R_{CP}^g is dominated in the resonance region by the contributions from Fig. 1(h). Since the complete expressions are rather lengthy we have split them with respect to the contributions from the individual diagrams. For example, $b_{g2}^{1(\text{h})}$ means the contribution from Fig. 1(h) to the function b_{g1}^{CP} and $c_{g1}^{1(\text{d}),(\text{e})}$ denotes the part of c_{g1} that is generated by the diagrams of Figs. 1(d) and 1(e).

The function b_{g1}^{CP} gets nonzero contributions only from the box diagrams of Fig. 1(c):

$$b_{g1}^{CP} = b_{g1}^{1(\text{c})} = \frac{m_t^3\sqrt{2}\,G_F\gamma_{CP}}{8\pi^2}\frac{-g_s^4 E_1}{96(-1+\beta^2 z^2)}$$

$$\times \{(7+9\beta z)[\text{Im}D_s(\hat{t})(1-\beta^2)-2\,\text{Im}D_{11}(\hat{t})\beta z E_1^2(1-\beta^2)+2(\text{Im}D_{11}(\hat{t})+\text{Im}D_{21}(\hat{t}))\beta^3 z E_1^2(z^2-1)] $$

$$+ (7-9\beta z)[-\text{Im}D_s(\hat{u})(1-\beta^2)-2\,\text{Im}D_{11}(\hat{u})\beta z E_1^2(1-\beta^2) $$

$$+ 2(\text{Im}D_{11}(\hat{u})+\text{Im}D_{21}(\hat{u}))\beta^3 z E_1^2(z^2-1)]\} . \tag{A17}$$

In this expression

$$D_s(\hat{t}) = D_0(\hat{t})(m_t^2-\hat{t})+C_0(\hat{s},m_\varphi^2,m_t^2,m_t^2), \quad D_s(\hat{u}) = D_0(\hat{u})(m_t^2-\hat{u})+C_0(\hat{s},m_\varphi^2,m_t^2,m_t^2) \tag{A18}$$

[where $C_0(\hat{s},m_\varphi,m_t,m_t)$ is defined in (A7)], $\hat{t} = (p_1-k_1)^2$, $\hat{u} = (p_2-k_1)^2$, and

$$D_0(\hat{t}); D_\mu(\hat{t}); D_{\mu\nu}(\hat{t}) = \int \frac{d^4 l}{i\pi^2} \frac{1; l_\mu; l_\mu l_\nu}{l^2 - m_\varphi^2 + i\epsilon} \frac{1}{(l+k_1)^2 - m_t^2 + i\epsilon} \frac{1}{(l+k_1-p_1)^2 - m_t^2 + i\epsilon} \frac{1}{(l+k_1-p_1-p_2)^2 - m_t^2 + i\epsilon} ,$$

$$D_\mu(\hat{t}) = D_{11}(\hat{t})k_{1\mu} - D_{12}(\hat{t})p_{1\mu} - D_{13}(\hat{t})p_{2\mu} ,$$

$$D_{\mu\nu}(\hat{t}) = D_{21}(\hat{t})k_{1\mu}k_{1\nu} + D_{22}(\hat{t})p_{1\mu}p_{1\nu} + D_{23}(\hat{t})p_{2\mu}p_{2\nu}$$

$$- D_{24}(\hat{t})k_{1\mu}p_{1\nu} - D_{25}(\hat{t})k_{1\mu}p_{2\nu} + D_{26}(\hat{t})p_{1\mu}p_{2\nu} + D_{27}(\hat{t})g_{\mu\nu} .$$

(A19)

$D_0(\hat{u}); D_\mu(\hat{u}); D_{\mu\nu}(\hat{u})$ are obtained from (A19) by interchanging p_1 and p_2. The functions $D_{11}, \ldots, D_{27}$ can be reduced to expressions which contain only the scalar two-, three-, and four-point functions B_0, C_0, D_0 (see, e.g., [39]).

The function b_{g2}^{CP} reads

$$b_{g2}^{CP} = b_{g2}^{1(c)} + b_{g2}^{1(g)} + b_{g2}^{1(h)} ,$$

$$b_{g2}^{1(c)} = \frac{m_t^3 \sqrt{2}\, G_F \gamma_{CP}}{8\pi^2} \frac{g_s^4 \beta}{96(-1+\beta^2 z^2)}$$

$$\times \left[(7+9\beta z) \left[-\text{Im}D_s(\hat{t})\frac{m_t}{E_1+m_t}(E_1+m_t+\beta z E_1) + 2\,\text{Im}D_{11}(\hat{t})m_t E_1(-E_1+E_1 z^2 - m_t z^2) + 4\,\text{Im}D_{27}(\hat{t})m_t \right. \right.$$

$$\left. + 2(\text{Im}(D_{11}\hat{t}) + \text{Im}D_{21}(\hat{t}))\beta^2 E_1^2(z^2-1)(2m_t + E_1 z^2 - m_t z^2) \right]$$

$$+ (7-9\beta z) \left[-\text{Im}D_s(\hat{u})\frac{m_t}{E_1+m_t}(E_1+m_t-\beta z E_1) + 2\,\text{Im}D_{11}(\hat{u})m_t E_1(-E_1+E_1 z^2 - m_t z^2) + 4\,\text{Im}D_{27}(\hat{u})m_t \right.$$

$$\left. \left. + 2(\text{Im}D_{11}(\hat{u}) + \text{Im}D_{21}(\hat{u}))\beta^2 E_1^2(z^2-1)(2m_t + E_1 z^2 - m_t z^2) \right] \right] ,$$

$$b_{g2}^{1(g)} = \frac{m_t^3 \sqrt{2}\, G_F \gamma_{CP}}{8\pi^2} \frac{3g_s^4 m_t \beta^3 z^2 \text{Im}G(\hat{s})}{8(-1+\beta^2 z^2)} ,$$

$$b_{g2}^{1(h)} = \frac{1}{(\hat{s}-m_\varphi^2)^2 + \Gamma_\varphi^2 m_\varphi^2} \frac{m_t^3 \sqrt{2}\, G_F \gamma_{CP}}{8\pi^2} \frac{g_s^4 m_t \beta}{4(-1+\beta^2 z^2)}$$

$$\times \{ 2m_t^2 [\text{Re}C_0(\hat{s}, m_t^2, m_t^2, m_t^2)\Gamma_\varphi m_\varphi - \text{Im}C_0(\hat{s}, m_t^2, m_t^2, m_t^2)(\hat{s}-m_\varphi^2)] + \Gamma_\varphi m_\varphi \} .$$

(A20)

As can be seen explicitly from these formulas, all contributions to the functions b_{g1}^{CP} and b_{g2}^{CP} result either from absorptive parts of the one-loop amplitudes or from terms of the form: width Γ_φ times dispersive terms (which is present only in $b_{g2}^{1(h)}$). This is in agreement with the general statements made in Sec. II. One can also check the relations following from Bose symmetry as given in Table I. The functions c_{g1} and c_{g2} arise from dispersive parts in the one-loop amplitude or width terms times absorptive parts (which is present only in $c_{g2}^{1(h)}$ below). They read

$$c_{g1} = c_{g1}^{1(c)} + c_{g1}^{1(d),(e)} + c_{g1}^{1(f)} ,$$

$$c_{g1}^{1(c)} = \frac{m_t^3 \sqrt{2}\, G_F \gamma_{CP}}{8\pi^2} \frac{-g_s^4 E_1}{96(-1+\beta^2 z^2)}$$

$$\times \{ (7+9\beta z)[\text{Re}D_s(\hat{t})(1-\beta^2) - 2\,\text{Re}D_{11}(\hat{t})\beta z E_1^2(1-\beta^2) - 2(\text{Re}D_{11}(\hat{t}) + \text{Re}D_{21}(\hat{t}))\beta^3 z E_1^2(z^2-1)]$$

$$+ (7-9\beta z)[-\text{Re}D_s(\hat{u})(1-\beta^2) - 2\,\text{Re}D_{11}(\hat{u})\beta z E_1^2(1-\beta^2) - 2(\text{Re}D_{11}(\hat{u}) + \text{Re}D_{21}(\hat{u}))\beta^3 z E_1^2(z^2-1)] \} ,$$

$$c_{g1}^{1(d),(e)} = \frac{m_t^3 \sqrt{2}\, G_F \gamma_{CP}}{8\pi^2} \frac{-g_s^4 E_1}{96(-1+\beta^2 z^2)}$$

$$\times \left[(9\beta z+7) \left[2C_0(\hat{t}, m_\varphi^2, m_t^2, m_t^2)(\beta^2-1) + \frac{\beta z}{\beta z - 1}C_s(\hat{t})(\beta^2 z^2 - 2\beta^2 + 1) \right] \right.$$

$$\left. + (9\beta z-7) \left[2C_0(\hat{u}, m_\varphi^2, m_t^2, m_t^2)(\beta^2-1) + \frac{\beta z}{\beta z + 1}C_s(\hat{u})(\beta^2 z^2 - 2\beta^2 + 1) \right] \right] ,$$

$$c_{g1}^{1(f)} = \frac{m_t^3 \sqrt{2}\, G_F \gamma_{CP}}{8\pi^2} \frac{-g_s^4}{192 E_1(-1+\beta^2 z^2)}$$

$$\times \left[(7+9\beta z)(B_0(m_t^2,m_\varphi^2,m_t^2) - B_0(\hat{t},m_\varphi^2,m_t^2)) \frac{\beta^2-1}{\beta z-1} + (7-9\beta z)(B_0(m_t^2,m_\varphi^2,m_t^2) - B_0(\hat{u},m_\varphi^2,m_t^2)) \frac{\beta^2-1}{\beta z+1} \right],$$

(A21)

where we used the notation

$$C_s(\hat{t}) = C_0(\hat{t},m_\varphi^2,m_t^2,m_t^2) + \frac{B_0(m_t^2,m_\varphi^2,m_t^2) - B_0(\hat{t},m_\varphi^2,m_t^2)}{m_t^2 - \hat{t}},$$

$$C_s(\hat{u}) = C_0(\hat{u},m_\varphi^2,m_t^2,m_t^2) + \frac{B_0(m_t^2,m_\varphi^2,m_t^2) - B_0(\hat{u},m_\varphi^2,m_t^2)}{m_t^2 - \hat{u}},$$

(A22)

and

$$C_0(\hat{t},m_\varphi^2,m_t^2,m_t^2) = \int \frac{d^4l}{i\pi^2} \frac{1}{l^2 - m_\varphi^2 + i\epsilon} \frac{1}{(l+k_1)^2 - m_t^2 + i\epsilon} \frac{1}{(l+k_1-p_1)^2 - m_t^2 + i\epsilon}.$$

(A23)

$C_0(\hat{u},m_\varphi^2,m_t^2,m_t^2)$ is obtained from (A23) by the replacement $p_1 \to p_2$. Finally,

$$c_{g2} = c_{g2}^{1(c)} + c_{g2}^{1(d),(e)} + c_{g2}^{1(f)} + c_{g2}^{1(g)} + c_{g2}^{1(h)},$$

$$c_{g2}^{1(c)} = \frac{m_t^3 \sqrt{2}\, G_F \gamma_{CP}}{8\pi^2} \frac{-g_s^4 \beta}{96(-1+\beta^2 z^2)}$$

$$\times \left[(7+9\beta z)\left[-\mathrm{Re}D_s(\hat{t})\frac{m_t}{E_1+m_t}(E_1+m_t-\beta z E_1) + 2\,\mathrm{Re}D_{11}(\hat{t})m_t E_1(E_1 - E_1 z^2 + m_t z^2) + 4\,\mathrm{Re}D_{27}(\hat{t})m_t \right.\right.$$

$$\left. + 2(\mathrm{Re}D_{11}(\hat{t}) + \mathrm{Re}D_{21}(\hat{t}))\beta^2 E_1^2(z^2-1)(2m_t + E_1 z^2 - m_t z^2) \right]$$

$$+ (7-9\beta z)\left[-\mathrm{Re}D_s(\hat{u})\frac{m_t}{E_1+m_t}(E_1+m_t+\beta z E_1) + 2\,\mathrm{Re}D_{11}(\hat{u})m_t E_1(E_1 - E_1 z^2 + m_t z^2) + 4\,\mathrm{Re}D_{27}(\hat{u})m_t \right.$$

$$\left.\left. + 2(\mathrm{Re}D_{11}(\hat{u}) + \mathrm{Re}D_{21}(\hat{u}))\beta^2 E_1^2(z^2-1)(2m_t + E_1 z^2 - m_t z^2) \right]\right],$$

$$c_{g2}^{1(d),(e)} = \frac{m_t^3 \sqrt{2}\, G_F \gamma_{CP}}{8\pi^2} \frac{-g_s^4 \beta}{96(-1+\beta^2 z^2)}$$

$$\times \left[(7+9\beta z)\left[2C_0(\hat{t},m_\varphi^2,m_t^2,m_t^2)\frac{m_t}{E_1+m_t}(E_1+m_t-\beta z E_1) + C_s(\hat{t})\frac{-m_t-E_1 z^2+m_t z^2}{E_1^2(1-\beta z)}(E_1^2 - 2m_t^2 - \beta^2 E_1^2 z^2) \right]\right.$$

$$+ (7-9\beta z)\left[2C_0(\hat{u},m_\varphi^2,m_t^2,m_t^2)\frac{m_t}{E_1+m_t}(E_1+m_t+\beta z E_1)\right.$$

$$\left.\left. + C_s(\hat{u})\frac{-m_t-E_1 z^2+m_t z^2}{E_1^2(1+\beta z)}(E_1^2 - 2m_t^2 - \beta^2 E_1^2 z^2) \right]\right],$$

$$c_{g2}^{1(f)} = \frac{m_t^3 \sqrt{2}\, G_F \gamma_{CP}}{8\pi^2} \frac{g_s^4 \beta}{192(-1+\beta^2 z^2)}$$

$$\times \left[(7+9\beta z)(B_0(m_t^2,m_\varphi^2,m_t^2) - B_0(\hat{t},m_\varphi^2,m_t^2))\frac{m_t}{E_1+m_t}\frac{E_1+m_t-\beta z E_1}{E_1^2(1-\beta z)} \right.$$

$$\left. + (7-9\beta z)(B_0(m_t^2,m_\varphi^2,m_t^2) - B_0(\hat{u},m_\varphi^2 m_t^2))\frac{m_t}{E_1+m_t}\frac{E_1+m_t+\beta z E_1}{E_1^2(1+\beta z)} \right],$$

$$c_{g2}^{1(g)} = \frac{m_t^3 \sqrt{2}\, G_F \gamma_{CP}}{8\pi^2} \frac{-3g_s^4 m_t \beta^3 z^2 \mathrm{Re}G(\hat{s})}{8(-1+\beta^2 z^2)},$$

$$c_{g2}^{1(h)} = \frac{g_s^4 \gamma_{CP}}{(\hat{s}-m_\varphi^2)^2+\Gamma_\varphi^2 m_\varphi^2} \left[-\frac{1}{16}\frac{m_t^3\sqrt{2}\,G_F}{8\pi^2}\frac{m_t\beta}{-1+\beta^2 z^2} \right.$$

$$\times \{2\hat{s}(1+\beta^2)[\mathrm{Re}C_0(\hat{s},m_t^2,m_t^2,m_t^2)(\hat{s}-m_\varphi^2)+\mathrm{Im}C_0(\hat{s},m_t^2,m_t^2,m_t^2)\Gamma_\varphi m_\varphi]-4(\hat{s}-m_\varphi^2)\}$$

$$\left. +\frac{3}{32}\left|\frac{m_t^3\sqrt{2}\,G_F}{8\pi^2}\right|^2 [2\hat{s}^3\beta\tilde{a}^2|C_0(\hat{s},m_t^2,m_t^2,m_t^2)|^2+2\hat{s}\beta a^2|2-\hat{s}\beta^2 C_0(\hat{s},m_t^2,m_t^2,m_t^2)|^2] \right].$$

(A24)

[1] L. Rolandi, in *Proceedings of the 26th International Conference on High Energy Physics,* Dallas, Texas, 1992, edited by J. Sanford, AIP Conf. Proc. No. 272 (AIP, New York, 1993), p. 56.

[2] CDF Collaboration, F. Abe *et al.,* in Proceedings of 16th International Symposium on Lepton and Photon Interactions, Ithaca, NY, 10-15 August 1993 (unpublished).

[3] M. Kobayashi and T. Maskawa, Prog. Theor. Phys. **49**, 652 (1973).

[4] N. Turok and J. Zadrozny, Nucl. Phys. **B358**, 471 (1991); L. McLerran, M. E. Shaposhnikov, N. Turok, and M. Voloshin, Phys. Lett. B **256**, 451 (1991); M. Dine, P. Huet, R. Singleton, and L. Susskind, *ibid.* **257**, 351 (1991); A. Nelson, A. Cohen, and D. Kaplan, Nucl. Phys. **B373**, 453 (1992).

[5] T. D. Lee, Phys. Rev. D **8**, 1226 (1973); Phys. Rep. **9**, 143 (1974); S. Weinberg, Phys. Rev. Lett. **37**, 657 (1976); P. Sikivie, Phys. Lett. B **B65**, 141 (1976); H. B. Lahanas, and C. E. Vayonakis, Phys. Rev. D **19**, 2158 (1979); G. C. Branco, A. J. Buras, and J. M. Gérard, Nucl. Phys. **B259**, 306 (1985); J. Liu and L. Wolfenstein, *ibid.* **B289**, 1 (1987).

[6] G. C. Branco and M. N. Revelo, Phys. Lett. **160B**, 117 (1985); S. Weinberg, Phys. Rev. D **42**, 860 (1990).

[7] N. G. Deshpande and E. Ma, Phys. Rev. D **16**, 1583 (1977).

[8] W. Bernreuther, T. Schröder, and T. N. Pham, Phys. Lett. B **279**, 389 (1992).

[9] B. Grzadkowski and J. Gunion, Phys. Lett. B **289**, 440 (1992).

[10] C. R. Schmidt and M. E. Peskin, Phys. Rev. Lett. **69**, 410 (1992).

[11] W. Bernreuther and A. Brandenburg, Phys. Lett. B **314**, 104 (1993).

[12] J. F. Donoghue and G. Valencia, Phys. Rev. Lett. **58**, 451 (1987); **59**, 243(E) (1988).

[13] C. A. Nelson, Phys. Rev. D **41**, 2805 (1990).

[14] W. Bernreuther and O. Nachtmann, Phys. Lett. B **268**, 424 (1991).

[15] G. L. Kane, G. A. Ladinsky, and C.-P. Yuan, Phys. Rev. D **45**, 124 (1991).

[16] W. Bernreuther, O. Nachtmann, P. Overmann, and T. Schröder, Nucl. Phys. **B388**, 53 (1992); **B406**, 516(E) (1993).

[17] D. Atwood and A. Soni, Phys. Rev. D **45**, 2405 (1992); D. Atwood, A. Aeppli, and A. Soni, Phys. Rev. Lett. **69**, 2754 (1992); D. Atwood, G. Eilam, and A. Soni, *ibid.* **71**, 492 (1993).

[18] J. P. Ma and A. Brandenburg, Z. Phys. C **56**, 97 (1992); A. Brandenburg and J. P. Ma, Phys. Lett. B **298**, 211 (1993).

[19] C. R. Schmidt, Phys. Lett. B **293**, 111 (1992).

[20] B. Grzadkowski, Phys. Lett. B **305**, 384 (1993); B. Grzadkowski and W.-Y. Keung, *ibid.* **316**, 137 (1993).

[21] W. Bernreuther and P. Overmann, Heidelberg Report No. HD-THEP-93-11, 1993 (unpublished).

[22] J. Liu, Phys. Rev. D **47**, R1741 (1993).

[23] A. Pilaftsis and M. Nowakoski, Mainz Report No. MZ-TH-92-56, 1992 (unpublished).

[24] D. Chang and W.-Y. Keung, Phys. Lett. B **305**, 261 (1993).

[25] D. Chang, W.-Y. Keung, and I. Phillips, Nucl. Phys. **B408**, 286 (1993).

[26] K. F. Smith *et al.,* Phys. Lett. B **234**, 191 (1990).

[27] S. A. Murthy *et al.,* Phys. Rev. Lett. **63**, 965 (1989); K. Abdullah *et al., ibid.* **65**, 2347 (1990).

[28] X. G. He, J. P. Ma, and B. McKellar, Melbourne Report No. UM-P-93-11, 1993 (unpublished); Phys. Lett. B **304**, 285 (1993).

[29] A. Mendez and A. Pomarol, Phys. Lett. B **272**, 313 (1991).

[30] J. F. Gunion, T. C. Yuan, and B. Grzadkowski, Phys. Rev. Lett. **71**, 488 (1993).

[31] A. Illakovac, B. A. Kniehl, and A. Pilaftsis, Phys. Lett. B **317**, 609 (1993).

[32] A. Djouadi and B. A. Kniehl, Report No. UDEM-LPN-TH-93-171, 1992 (unpublished).

[33] C.Kao, Florida Report No. FSU-HEP-930924, 1993 (unpublished).

[34] J. Kühn, Acta Phys. Austriaca Suppl. XXIV, 203 (1982); I. Bigi, Y. Dokshitzer, V. Khoze, J. Kühn, and P. Zerwas, Phys. Lett. B **181**, 157 (1986).

[35] A. Czarnecki, M. Jezabek, and J. H. Kühn, Nucl. Phys. **B351**, 70 (1991).

[36] G. A. Ladinsky, Phys. Rev. D **46**, 3789 (1992); **47**, 3086(E) (1993).

[37] J. F. Owens, Phys. Lett. B **266**, 126 (1991).

[38] G. 't Hooft and M. Veltman, Nucl. Phys. **B153**, 365 (1979).

[39] G. Pasarino and M. Veltman, Nucl. Phys. **B160**, 151 (1979).